Published in final edited form as:
Bone. 2010 April ; 46(4): 1131–1137. doi:10.1016/j.bone.2009.12.026.

FUNCTIONAL AND ASSOCIATION ANALYSIS OF FRIZZLED 1 (FZD1) PROMOTER HAPLOTYPES WITH FEMORAL NECK GEOMETRY

Yingze Zhang, Ph.D.[1,3,4], **Allison L. Kuipers, B.S.**[2,*], **Laura M. Yerges-Armstrong, Ph.D.**[2,*], **Cara S. Nestlerode, M.S.**[2], **Zhao Jin, M.S.**[1], **Victor W. Wheeler, M.D.**[5], **Alan L. Patrick, M.D.**[5], **ClareAnn H. Bunker, Ph.D.**[2], and **Joseph M. Zmuda, Ph.D**[2,3]

[1] Division of Pulmonary, Allergy, and Critical Care Medicine, Department of Medicine, University of Pittsburgh, Pittsburgh, PA

[2]Department of Epidemiology, University of Pittsburgh, Pittsburgh, PA

[3]Department of Human Genetics, University of Pittsburgh, Pittsburgh, PA

[4]Dorothy P. & Richard P. Simmons Center for Interstitial Lung Disease, University of Pittsburgh, Pittsburgh, PA

[5]Tobago Health Studies Office, Scarborough, Tobago

Abstract

Frizzleds are receptors for Wnt signaling and are involved in skeletal morphogenesis. Little is known about the transcriptional regulation of frizzleds in bone cells. In the current study, we determined if two common and potentially functional genetic variants (rs2232157, rs2232158) in the frizzled-1 (*FZD1*) promoter region and their haplotypes influence *FZD1* promoter activity in human osteoblast-like cells. We also determined if these variants are associated with femoral neck bone mineral density (BMD) and geometry in 1319 African ancestry men aged ≥40 years. Real-time quantitative PCR and western blot analysis demonstrated FZD1 mRNA and protein expression in the human osteoblast-like cell lines, MG63 and SaOS-2. Promoter activity was next assessed by transient expression of haplotype specific *FZD1* promoter reporter plasmids in these cells. In comparison to the common GG haplotype, promoter activity was 3-fold higher for the TC haplotype in both cell lines ($p<0.05$). We previously demonstrated that rs2232158 is associated with differential *FZD1* promoter activity and Egr1 binding and thus focused further functional analyses on the rs2232157 G-to-T polymorphism. Electrophoretic mobility shift assay demonstrated that distinct nuclear protein complexes were associated with rs2232157 in an allele specific manner. Bioinformatics analysis predicted that the G to T transversion creates an E2F1 binding site, further supporting the functional significance of rs2232157 in *FZD1* promoter regulation. Individual SNPs and haplotypes were not associated with femoral neck BMD. The TC haplotype was associated with larger subperiosteal width and greater CSMI ($p<0.05$). These results suggest that FZD1 expression is regulated in a haplotype

Address correspondence to: Yingze Zhang , Department of Medicine, School of Medicine, University of Pittsburgh, NW628 MUH, 3459 Fifth Avenue, Pittsburgh, PA 15213, Phone 412-692-2306, Fax 412-692-2260, zhangy@upmc.edu ; or Joseph Zmuda, Department of Epidemiology, Graduate School of Public Health, University of Pittsburgh, 130 DeSoto Street, Pittsburgh, PA 15261, Phone: 412-624-2970, Fax: 412-624-7397, zmudaj@edc.pitt.edu.
*These authors contributed equally to the present work.

dependent manner in osteoblasts and that these same haplotypes may be associated with biomechanical indices of bone strength.

Keywords

frizzled-1; haplotype; osteoblast; WNT; osteoporosis

Introduction

The wingless-type MMTV integration site (Wnt)/β-catenin signaling pathway has emerged as an important regulator of skeletal development [1-3]. Osteoblasts are responsible for bone formation and osteoblast differentiation, proliferation and apoptosis is regulated by the Wnt signaling [1,2,4]. Wnts bind to a cell surface receptor complex consisting of LRP5 and its co-receptor frizzled (FZD) to initiate canonical signal transduction [4,5]. Frizzleds may also signal through the noncanonical planar cell polarity (PCP) pathway, which controls polarized cell movements and the establishment of tissue polarity [6-8], the ROR2/RYK coreceptors to the dishevelled-dependent or the Ca(2+)-dependent signaling cascades [9-12]. Wnt signals are context-dependent based on the expression profile of frizzled receptors and other extracellular and intracellular Wnt signaling regulators. Very little is currently known about the regulation of frizzled receptors, particularly in bone cells.

Bone strength and the risk of osteoporotic fracture are determined to some extent by bone mineral density (BMD). However, BMD is not the only determinant of bone strength and fracture risk. The structural geometric properties of bone, such as the size, thickness, shape and spatial distribution of bone mass in cross-section, may also influence bone strength and fracture propensity [13,14,15,16]. For example, the ability of long bone diaphyses to resist bending and twisting depends on how the cortical area (and bone mass) is distributed about the center of the diaphysis, a geometric property known as the cross-sectional moment of inertia [17]. Bone mass distributed further from the center of the diaphysis (i.e., bone added to the periosteal or outer surface) is more effective in resisting bending and twisting forces than bone mass added to the inner (endosteal) surface [17]. The external diameter of bone is exponentially related to bone strength such that even small contributions to bone circumference add considerably to its strength [18]. Reduced periosteal bone formation is thought to be a major mechanism contributing to deficits in bone size and increased skeletal fragility in growth and aging [18-22]. Racial differences in skeletal geometry may also have important effects on fracture epidemiology [23]. Skeletal geometry also has a strong and poorly understood genetic foundation [24,25].

Mutations in the Wnt co-receptor LRP5 are an established cause of rare high and low BMD and common variants in LRP5 are also associated with normal variation in BMD [26,27,28]. We recently reported a novel association of common promoter variants in the frizzled 1 (FZD1) co-receptor with skeletal geometry [29]. In the current study, we extend these findings by analyzing the individual and multi-site promoter haplotypes with the geometric characteristics of the femoral neck, a clinically important skeletal site, in a large sample of Afro-Caribbean men. We also examined the effects of the individual SNPs and haplotypes on *FZD1* promoter activity in human osteoblast-like cells. Our results indicate that FZD1 expression is regulated in a SNP and haplotype dependent manner in osteoblast-like cells and that these same variants are associated with biomechanical indices of bone strength, providing further evidence for an impact of FZD1 genetic variation on bone biology.

Methods

Study Population

The population-based Tobago Bone Health Study was initially conducted on the Caribbean island of Tobago in 2000 [30,31]. In brief, recruitment was accomplished by word of mouth, hospital flyers and radio broadcasting. To be eligible, men had to be 40 years and older, ambulatory and not terminally ill. Questionnaires were administered to obtain information on demographic characteristics, occupation, medical history, and lifestyle related factors. A total of 2,652 men completed an initial dual-energy x-ray aborptiometry (DXA) scan for assessment of BMD. Self-reported ethnicity of the cohort is 97% African, 2% East Indian, <1% white, and <1% "other". We excluded men who identified themselves with ethnicity other than Afro-Caribbean for the current analysis. The final dataset for the current analysis consisted of 1319 men with proximal femur geometry measurements from DXA scans. Their mean age was 59.78 years. The Institutional Review Boards of the University of Pittsburgh and the Tobago Ministry of Health and Social Services approved this study and all participants provided written informed consent before data collection.

Densitometry

Each participant received a single hip and total body scan with a Hologic QDR 4500 dual energy x-ray absorptiometry DXA scanner using the array beam mode (Hologic Inc. Bedford, MA, USA). Standardized procedures for participant positioning and scan analysis were followed according to the manufacturer's recommended protocol. Scans were analyzed with QDR software version 8.26a. Hip scans were further analyzed with the Hip Structural Analysis (HSA) program developed by Beck et al [16].

Hip Structural Analysis (HSA)

The HSA program employs conventional DXA image data to derive geometric properties of bone cross-sections. The program uses the distribution of mineral mass in a line of pixels traversing the bone axis to describe the geometry of the corresponding cross-section at that point. For precision, measurements are averaged over 5 parallel lines (5 mm) across the bone axis. Geometric properties are measured for cross-sections in cut planes traversing the narrowest point of the femoral neck at a distance 1.5 times the measured neck subperiosteal width, distal to intersection of the neck and shaft axes. Cross-sectional moment of inertia (I_x) for bending in the image plane from bone mass profile integral was defined as:

$$I_x = \frac{x_p}{\rho_{be}} \Sigma (y - y_c)^2 m_{bi}$$

where x_p is the pixel spacing along the bone mass profile, m_{bi} is the pixel value in g/cm^2 of the ith pixel, ρ_{be} is the effective density of bone mineral in bone tissue, and y is the locus of the current pixel and y_c is the locus of the center of mass of the profile. Conventional areal BMD (g/cm^2), bone cross-sectional area (CSA, cm^2), subperiosteal width (cm) and section modulus (cm^3) were measured directly from the bone profile using algorithms described previously [16]. Bone CSA is equivalent to the amount of bone surface area in the cross-section after excluding soft tissue space and is proportional to conventional bone mineral content (BMC, g). Bone CSA is an indicator of bone axial strength in compression. Section modulus (cm^3) was calculated as cross-sectional moment of inertia divided by the distance from the center of mass to the medial or lateral surface (whichever is greater).

Other Measurements

Height was measured to the nearest 0.1 cm using a wall-mounted stadiometer. Weight was recorded to the nearest 0.1 kg without shoes on a balance beam scale. Body mass index was calculated as weight in kg divided by height in meters squared.

Genotyping

Genomic DNA was isolated from either whole blood extracted by the salting out method or from blood clots collected in coagulation tubes and isolated by a Qiagen column procedure (Qiagen, Santa Clara, CA). Two of the common variants rs2232157 and rs2232158 in the *FZD1* promoter region were genotyped using direct DNA sequencing and carried out by DNA Polymorphic (Alameda, CA) on the ABI 3730XL DNA Analyzer (Applied Biosystems, Foster City, CA). Sequence analysis and variant detection were completed with Sequencher 4.9 sequence analysis software (Genecodes, Ann Arbor, MI). Genotypes were validated with both forward and reverse sequencing fragments. There was a >99% genotype completeness rate.

Cell Culture

The human osteoblast-like cell lines MG63 and SaOS-2 were cultured in RPMI medium 1640 with L-Glutamine and 10% fetal bovine serum (v/v) (Invitrogen; Carlsbad, CA). Penicillin/Streptomycin was included in all culture media at a concentration of 2units/mL. The cell cultures were maintained at 37°C in a humidified chamber with 5% CO_2.

Real-time Quantitative PCR

The human osteoblast-like cell lines MG63 and SaOS-2 were cultured to subconfluence (~80-90%) and used for total RNA isolation with Trizol reagent (Invitrogen, Carlsbad, CA) according to the manufacturer's instructions. Total RNA samples were analyzed using a Nanodrop spectrophotometer (Nanodrop Products, Wilmington, DE). Reverse transcription and real time quantitative PCR were performed using *FZD1* primer/probes (Hs00268943_s1, Applied Biosystems. Foster City, CA) as described previously [32]. *FZD1* expression was normalized to human *GAPDH* expression level. All reactions were run in duplicate. No template and no reverse transcriptase controls were performed simultaneously. Relative expression of FZD1 was determined by the change of cycle threshold (ΔCt) between the FZD1 and the internal control GAPDH. It was calculated as $\Delta Ct = Ct^{FZD1}\text{-}Ct^{GAPDH}$ for each cell line.

Western Blot Analysis

Ten micrograms of total protein isolated from cells at subconfluence were resolved by SDS-PAGE, transferred to nitrocellulose membrane and analyzed by standard immunoblotting using HRP-conjugated secondary antibody and chemiluminescence detection (Pierce Biotechnology, Rockford, IL). Rabbit polyclonal anti-FZD1 antibody was used (AP-2755b Abgent, San Diego, CA).

Electrophoretic Mobility Shift Assay (EMSA)

Nuclear extracts for EMSAs were prepared from MG63 and SaOS-2 cells using the Nuclear Extraction Kit (Active Motif, Carlsbad, CA). EMSA was performed using ^{32}P (5′-end)-labeled double-stranded oligonucleotides specific for the two alleles of rs2232157 (5′-GACCCCGGCGCGCCC(G/T)AGCCACCC G-3′) as described previously [29].

Generation of FZD Promoter Luciferase Reporter Constructs

Haplotype specific *FZD1* promoter region constructs encompassing the rs2232157 and the rs2232158 SNPs were generated using genomic DNA from individuals with the haplotypes of

interest. A 726 bp fragment spanning −655 to +71 nucleotide relative to the translation start point was cloned into the pGL3 basic vector (Promega, Madison WI). Direct DNA sequencing was used to verify the *FZD1* inserts in the pGL3 basic vector. The cloning strategy and experimental design were described in detail previously [29].

Promoter Activity Analysis

The MG63 and SaOS-2cells were seeded in 48 well culture plates 24 hr prior to transfection to obtain sub-confluence (~70-80%) at the time of transfection. Transfection was performed using Lipofectamine LTX (Invitrogen; Carlsbad, California). The cells were harvested at 30-36 hours post-transfection and firefly luciferase activities were analyzed using the luciferase assay system (Promega, Madison WI). Six replicates for each experimental condition were included.

In silico functional analysis

We used Transcription Element Search Software (TESS: http://www.cbil.upenn.edu/tess) to assess the potential functional significance of rs2232157.

Statistical Analysis

We calculated site-specific allele frequencies by gene counting and tested for departures from Hardy-Weinberg equilibrium using a goodness of fit statistic. Pairwise estimates of linkage disequilibrium were measured as D′ and r^2 from the diploid data [33].

In the population study, single SNPs were tested for their association with bone parameters. Linear regression was used to test for association between the number of rare alleles and the bone parameters. Analysis of covariance was used to assess dominant and recessive models. All models were adjusted for age, height and weight and the adjusted, genotype-specific means and standard errors are presented. Analyses were performed using SAS version 9.1 (SAS Institute, Cary, NC).

To conduct the haplotype analysis, we used PHASE (version 2.1) [34] to infer haplotypes from the unphased SNPs and coded the resulting haplotypes according to the number of copies present for each participant. We excluded any haplotypes with an estimation probability less than 90% confidence (n=2), giving a final sample of 1317 individuals for the haplotype analyses. Haplotype associations with bone parameters were completed in the same manner as single SNP analyses adjusting for age, height and weight.

Non-parametric statistical methods were used to analyze the functional data. Specifically, the Kruskal-Wallis test and the Wilcoxon rank-sum test were used to assess the significance of differential promoter activities associated with haplotype specific reporter plasmids in the transfection experiment.

Results

FZD1 Expression in Human Osteoblast-like Cells

We first characterized the expression levels of FZD1 mRNA and protein using the osteoblast-like cell lines, MG63 and SaOS-2. Using real time quantitative RT-PCR, FZD1 expression was detected in both cell lines with relatively higher levels in the MG63 cells (Figure 1b). The presence of FZD1 in these cells was further confirmed using western blot analysis. In agreement with the real time quantitative RT-PCR, FZD1 protein was detected in both cells and the expression level was higher in the MG63 cells (Figure 1c).

Haplotype Specific Promoter Activity of FZD1 in Osteoblast-like cells

To assess whether the promoter haplotypes influence the transcription of *FZD1* in osteoblasts, haplotype specific promoter constructs were generated and analyzed in MG63 and SaOS-2 cells (Figure 1d). Promoter activity was assessed by transient expression of haplotype specific *FZD1* promoter reporter plasmids in the cell lines. Since one of the four possible haplotypes, TG, was not observed in our study sample, the functional analysis was focused on the three haplotypes: GG, GC and TC. A significant difference among haplotypes was observed in MG63 and SaoS-2 cells ($p<0.05$ for both cases). The most common GG haplotype exhibited the lowest promoter activity while the TC haplotype carrying both minor alleles resulted in the strongest promoter activity in both cell lines. In comparison to the GG haplotype, the promoter activity was 2.28 and 3.05 fold higher for the GC and TC haplotypes in MG63 cells ($p< 0.05$ for both haplotypes). Similarly, greater promoter activity was detected for GC and TC haplotypes in comparison to the GG haplotype in SaoS-2 cells (3.36 and 3.66 fold, respectively; $p=0.0051$ for both comparisons).

Allele Specific Nuclear Protein Complexes for rs2232157

We previously demonstrated that rs2232158 is associated with differential *FZD1* promoter activity and with allele specific Egr1 binding [29]. Thus in the current study, we only examined the potential impact of rs2232157 on transcription factor binding. The higher promoter activity observed for the TC haplotype than the GC haplotype suggested a potential functional role for rs2232157 in the transcriptional regulation of the *FZD1* gene. To explore whether the rs2232157 G-to-T polymorphism alters transcription factor binding, an EMSA was completed (Figure 1e). Nuclear protein extracts from MG63 and SaOS-2 cells were used with allele specific oligonucleotides containing the rs2232157 site. Two nuclear complexes (labeled as A and B) were specific and allele dependent. Complex A was primarily observed in the G specific probe with much less observed in the T specific probe. In contrast, complex B was only detected in the T specific probe and not in the G specific probe. The allele dependent complex formation was further supported by the specific competition of each complex with 50-fold unlabeled allele specific probes. The rs2232157G probe was only able to compete with complex A, while complex B was competed out by the rs2232157T probe. Therefore, transcription factor binding was altered due to the G-to-T polymorphism for rs2232157. Furthermore, bioinformatics analysis using TESS indicates that rs2232157 may alter E2F1 binding such that the T allele creates a binding site for EIIaE-A, a homolog of E2F1 (Transcription Element Search Software http://www.cbil.upenn.edu/tess).

Allele and Haplotype Population Frequencies

Based on our previous report, we focused on the two common promoter SNPs, rs2232157 and rs2232158 (Figure 1a). The observed MAFs were 21% for rs2232157 and 34% for rs2232158 (Table 1). Both SNPs met the expectations of Hardy-Weinberg equilibrium ($p>0.01$). The two SNPs were in linkage disequilibrium ($r^2=0.671$; $D'=1.0$).

Haplotype estimation predicted three haplotypes: GG, GC and TC with a frequency of 71.8%, 6.9% and 21.3%, respectively (Table 1). The TG haplotype was not observed in this study sample. The absence of this haplotype was further verified with haplotype specific cloning using DNA samples of the GT/GC genotype combinations. DNA from 5 individuals who were heterozygous for both SNPs was cloned into pGEMTeasy vector and a minimum of 3 clones were sequenced. We did not detect the TG haplotype in any of the clones tested from these samples.

Association of the FZD1 Promoter Variants with Femoral Neck Geometry

We analyzed the association of FZD1 promoter variants with femoral neck geometry using both dominant and recessive models and the dominant model was the best fitting model for this analysis. Bone mineral density and cross-sectional area of the femoral neck were not associated with either of the *FZD1* polymorphisms (Table 2). However, presence of the T allele at rs2232157 was associated with a 0.28 mm increase in subperiosteal width (p=0.017). The femoral neck in individuals with the T allele was also significantly stronger, assessed via cross-sectional moment of inertia, than those with the G allele (p=0.030). In contrast, presence of the C allele at rs2232158 was associated with a 0.25 mm decrease in subperiosteal width (p=0.038). In addition, the femoral neck of the individuals with the C allele tended to be weaker, as assessed via cross-sectional moment of inertia, than those with the G allele, although the association did not quite achieve statistical significance (p=0.059).

Association of the FZD1 Promoter Haplotypes with Femoral Neck Geometry

Haplotypes of *FZD1* promoter polymorphisms were not associated with femoral neck BMD or CSA, similar to results for the individual SNPs (Table 3). Under a recessive model, individuals with two copies of the wildtype haplotype (GG) had smaller subperiosteal width and lower cross-sectional moment of inertia compared to individuals with zero or one copy of the haplotype (p=0.026 and p=0.031, respectively). Under a dominant model, individuals with at least one copy of the TC haplotype had larger subperiosteal width and greater CSMI (p=0.018 and p=0.029, respectively).

Discussion

Frizzled co-receptors appear to play a role in the maturation of the periosteum and the three-dimensional morphogenesis of the skeleton [8,35]. In order to better understand the potential influence of *FZD1* polymorphisms on its transcriptional regulation and bone mass and skeletal geometry in humans, we characterized haplotype specific promoters in osteoblast-like cells and conducted genetic association analyses of two previously identified promoter polymorphisms (rs2232157, rs2232158) [29] and their haplotypes in a large population cohort of African ancestry men. Transient expression of the haplotype specific promoters in human osteoblast-like cells demonstrated significantly different promoter activities. Furthermore, we observed a significant association between the individual polymorphisms and their haplotypes with the subperiosteal width and cross-sectional moment of inertia at the femoral neck but not with BMD. This finding, in combination with our previous report [29], suggests that rs2232157 and rs2232158 in the *FZD1* promoter region and their haplotypes may be functionally important in regulating the transcription of *FZD1* in osteoblasts and are also associated with bone size and biomechanical indices of bone strength. These data provide further evidence for the potential impact of *FZD1* genetic variation on individual differences in skeletal morphology.

Direct comparison of the GG and GC haplotypes showed stronger promoter activity for the GC specific construct. This was consistent with our previous demonstration that the rs2232158C allele is associated with Egr1 dependent transactivation of the *FZD1* promoter [29]. The promoter activity was further enhanced in the TC haplotype compared to the GC haplotype suggesting additional rs2232157T dependent transcriptional activation of the *FZD1* gene. This finding was supported by the differential binding of nuclear proteins to the rs2232157G and T alleles as demonstrated in the EMSA analysis (Figure 1e) and by the *in silico* prediction that the G to T transversion creates an E2F1 binding site. The E2F proteins bind DNA cooperatively with co- regulatory factors through the E2 recognition site found in the promoter region of many E2F target genes involved in cell cycle regulation or in DNA replication [36,37,38]. E2F proteins play important roles in controlling cellular proliferation

and development [39,40]. The role of E2F in bone development was demonstrated in E2F1 and E2F3 double knockout mice which developed deficits in long bone size [41]. Moreover, E2F1 transgenic mice have delayed endochondral ossification, which is especially important for longitudinal bone growth of the limbs [42]. E2F1 has also been shown to repress the Wnt/β-catenin pathway and serves as a point of cross-talk between the Wnt/β-catenin and pRb/E2F pathways in cancer [43]. Further studies are needed to determine if E2F1 directly binds to the *FZD1* promoter region and is differentially influenced by *FZD1* promoter polymorphisms and/or haplotypes in both osteoblasts and chondyocytes.

Osteoporotic fractures are associated with BMD but other indices of bone strength, such as skeletal geometry, also appear to influence fracture risk [44,45,46]. While the heritability and genetics of BMD has been widely studied, much less is known about the genetic influences on bone geometry. Femoral neck geometric properties are highly heritable [24,25] but the genetic loci influencing skeletal geometry are largely unknown. In the current analysis, we did not observe an association between *FZD1* promoter polymorphisms or haplotypes and femoral neck BMD suggesting that *FZD1* genetic variants may influence bone size and the spatial distribution of bone mineral but not mineral density. Our findings in humans are consistent with experimental studies in chickens that demonstrate an important role of Wnt and frizzled signaling on bone size [8,35]. Also consistent with our observations, a recent study in 371 postmenopausal Korean women found no association between a *FZD1* coding polymorphism and DXA measures of BMD, although this study did not specifically analyze rs2232158 or rs2232157 [47]. Previous genome-wide association studies of BMD have also not demonstrated an association between polymorphisms within or flanking *FZD1* and BMD in mixed samples of largely Caucasian men and women [48-52]. However, the genome-wide SNP chips used in these studies did not include rs2232158 or rs2232157 and had few other SNPs within the *FZD1* gene region (http://genome.ucsc.edu).

Our analysis was limited to Afro-Caribbean men and our findings may not be generalizable to other populations. In addition, our study was designed to investigate common variation in the *FZD1* promoter region and its association on skeletal traits and we cannot exclude the possibility that low frequency or rare variants within the coding region of *FZD1* impacts BMD or skeletal geometry. However, we only focused on two potentially functional variants in the proximal promoter region and cannot exclude the likelihood that more distal regulatory variants are also associated with bone phenotypes. Finally, we only analyzed the *FZD1* promoter in osteoblast-like cells and characterization of the *FZD1* promoter in other cell types, in particular, chondrocytes will be necessary to understand the complex role of FZD1 in bone biology.

In conclusion, Wnt signaling is important in skeletal development and several Wnt related genes have already been implicated in the regulation of the skeletal phenotype. The current analysis provides additional evidence that common and potentially functional genetic variants in the promoter region of the Wnt co-receptor, frizzled-1, may contribute, in part, to the heritable influence on skeletal geometry. Moreover, our functional analysis also supports a role of promoter variants and haplotypes in the regulation of FZD1 expression in osteoblast-like cells.

Acknowledgments

The authors thank Dr. Yanxia Chu for technical assistance in Western blot analysis. This study was supported, in part, by grants R01-AR049747 from the National Institute of Arthritis and Musculoskeletal and Skin Diseases and funding from the National Osteoporosis Foundation and Western Pennsylvania Arthritis Foundation. Laura M. Yerges-Armstrong, Ph.D. was supported by National Institute of Aging grant T32-AG00181. Allison Kuipers, B.S. was supported by National Heart Lung and Blood Institute Grant T32-HL083825.

References

1. Hartmann C. A Wnt canon orchestrating osteoblastogenesis. Trends Cell Biol 2006;16:151–8. [PubMed: 16466918]
2. Westendorf JJ, Kahler RA, Schroeder TM. Wnt signaling in osteoblasts and bone diseases. Gene 2004;341:19–39. [PubMed: 15474285]
3. Baron R, Rawadi G, Roman-Roman S. Wnt signaling: a key regulator of bone mass. Curr Top Dev Biol 2006;76:103–27. [PubMed: 17118265]
4. He X, Semenov M, Tamai K, Zeng X. LDL receptor-related proteins 5 and 6 in Wnt/beta-catenin signaling: arrows point the way. Development 2004;131:1663–77. [PubMed: 15084453]
5. Umbhauer M, Djiane A, Goisset C, Penzo-Mendez A, Riou JF, Boucaut JC, Shi DL. The C-terminal cytoplasmic Lys-thr-X-X-X-Trp motif in frizzled receptors mediates Wnt/beta-catenin signalling. EMBO J 2000;19:4944–54. [PubMed: 10990458]
6. Seifert JR, Mlodzik M. Frizzled/PCP signalling: a conserved mechanism regulating cell polarity and directed motility. Nat Rev Genet 2007;8:126–38. [PubMed: 17230199]
7. Doyle K, Hogan J, Lester M, Collier S. The Frizzled Planar Cell Polarity signaling pathway controls Drosophila wing topography. Dev Biol 2008;317:354–67. [PubMed: 18384764]
8. Li Y, Dudley AT. Noncanonical frizzled signaling regulates cell polarity of growth plate chondrocytes. Development 2009;136:1083–92. [PubMed: 19224985]
9. Lu W, Yamamoto V, Ortega B, Baltimore D. Mammalian Ryk is a Wnt coreceptor required for stimulation of neurite outgrowth. Cell 2004;119:97–108. [PubMed: 15454084]
10. Oishi I, Suzuki H, Onishi N, Takada R, Kani S, Ohkawara B, Koshida I, Suzuki K, Yamada G, Schwabe GC, Mundlos S, Shibuya H, Takada S, Minami Y. The receptor tyrosine kinase Ror2 is involved in non-canonical Wnt5a/JNK signalling pathway. Genes Cells 2003;8:645–54. [PubMed: 12839624]
11. Katoh M. WNT signaling pathway and stem cell signaling network. Clin Cancer Res 2007;13:4042–5. [PubMed: 17634527]
12. Dejmek J, Safholm A, Kamp Nielsen C, Andersson T, Leandersson K. Wnt-5a/Ca2+-induced NFAT activity is counteracted by Wnt-5a/Yes-Cdc42-casein kinase 1alpha signaling in human mammary epithelial cells. Mol Cell Biol 2006;26:6024–36. [PubMed: 16880514]
13. Martin B. Aging and strength of bone as a structural material. Calcif Tissue Int 1993;53(Suppl 1):S34–9. discussion S39-40. [PubMed: 8275378]
14. Peacock M, Turner CH, Liu G, Manatunga AK, Timmerman L, Johnston CC Jr. Better discrimination of hip fracture using bone density, geometry and architecture. Osteoporos Int 1995;5:167–73. [PubMed: 7655177]
15. Gluer CC, Cummings SR, Pressman A, Li J, Gluer K, Faulkner KG, Grampp S, Genant HK. Prediction of hip fractures from pelvic radiographs: the study of osteoporotic fractures. The Study of Osteoporotic Fractures Research Group. J Bone Miner Res 1994;9:671–7. [PubMed: 8053396]
16. Beck TJ, Ruff CB, Warden KE, Scott WW Jr. Rao GU. Predicting femoral neck strength from bone mineral data. A structural approach. Invest Radiol 1990;25:6–18. [PubMed: 2298552]
17. Martin, RB. Aging and changes in cortical mass and structure. In: Orwoll, E., editor. Osteoporosis in Men. Academic Press; San Diego: 1999. p. 111-128.
18. Orwoll ES. Toward an expanded understanding of the role of the periosteum in skeletal health. J Bone Miner Res 2003;18:949–54. [PubMed: 12817746]
19. Tabensky A, Duan Y, Edmonds J, Seeman E. The contribution of reduced peak accrual of bone and age-related bone loss to osteoporosis at the spine and hip: insights from the daughters of women with vertebral or hip fractures. J Bone Miner Res 2001;16:1101–7. [PubMed: 11393787]
20. Duan Y, Turner CH, Kim BT, Seeman E. Sexual dimorphism in vertebral fragility is more the result of gender differences in age-related bone gain than bone loss. J Bone Miner Res 2001;16:2267–75. [PubMed: 11760841]
21. Duan Y, Seeman E, Turner CH. The biomechanical basis of vertebral body fragility in men and women. J Bone Miner Res 2001;16:2276–83. [PubMed: 11760842]
22. Seeman E. During aging, men lose less bone than women because they gain more periosteal bone, not because they resorb less endosteal bone. Calcif Tissue Int 2001;69:205–8. [PubMed: 11730251]

23. Seeman E. The structural basis of bone fragility in men. Bone 1999;25:143–7. [PubMed: 10423041]
24. Streeten EA, Beck TJ, O'Connell JR, Rampersand E, McBride DJ, Takala SL, Pollin TI, Uusi-Rasi K, Mitchell BD, Shuldiner AR. Autosome-wide linkage analysis of hip structural phenotypes in the Old Order Amish. Bone 2008;43:607–12. [PubMed: 18555766]
25. Demissie S, Dupuis J, Cupples LA, Beck TJ, Kiel DP, Karasik D. Proximal hip geometry is linked to several chromosomal regions: genome-wide linkage results from the Framingham Osteoporosis Study. Bone 2007;40:743–50. [PubMed: 17079199]
26. Ferrari SL, Deutsch S, Choudhury U, Chevalley T, Bonjour JP, Dermitzakis ET, Rizzoli R, Antonarakis SE. Polymorphisms in the low-density lipoprotein receptor-related protein 5 (LRP5) gene are associated with variation in vertebral bone mass, vertebral bone size, and stature in whites. Am J Hum Genet 2004;74:866–75. [PubMed: 15077203]
27. Koller DL, Ichikawa S, Johnson ML, Lai D, Xuei X, Edenberg HJ, Conneally PM, Hui SL, Johnston CC, Peacock M, Foroud T, Econs MJ. Contribution of the LRP5 gene to normal variation in peak BMD in women. J Bone Miner Res 2005;20:75–80. [PubMed: 15619672]
28. van Meurs JB, Trikalinos TA, Ralston SH, Balcells S, Brandi ML, Brixen K, Kiel DP, Langdahl BL, Lips P, Ljunggren O, Lorenc R, Obermayer-Pietsch B, Ohlsson C, Pettersson U, Reid DM, Rousseau F, Scollen S, Van Hul W, Agueda L, Akesson K, Benevolenskaya LI, Ferrari SL, Hallmans G, Hofman A, Husted LB, Kruk M, Kaptoge S, Karasik D, Karlsson MK, Lorentzon M, Masi L, McGuigan FE, Mellstrom D, Mosekilde L, Nogues X, Pols HA, Reeve J, Renner W, Rivadeneira F, van Schoor NM, Weber K, Ioannidis JP, Uitterlinden AG. Large-scale analysis of association between LRP5 and LRP6 variants and osteoporosis. JAMA 2008;299:1277–90. [PubMed: 18349089]
29. Yerges LM, Zhang Y, Cauley JA, Kammerer CM, Nestlerode CS, Wheeler VW, Patrick AL, Bunker CH, Moffett SP, Ferrell RE, Zmuda JM. Functional characterization of genetic variation in the Frizzled 1 (FZD1) promoter and association with bone phenotypes: more to the LRP5 story? J Bone Miner Res 2009;24:87–96. [PubMed: 18715140]
30. Bunker CH, Patrick AL, Konety BR, Dhir R, Brufsky AM, Vivas CA, Becich MJ, Trump DL, Kuller LH. High prevalence of screening-detected prostate cancer among Afro-Caribbeans: the Tobago Prostate Cancer Survey. Cancer Epidemiol Biomarkers Prev 2002;11:726–9. [PubMed: 12163325]
31. Hill DD, Cauley JA, Bunker CH, Baker CE, Patrick AL, Beckles GL, Wheeler VW, Zmuda JM. Correlates of bone mineral density among postmenopausal women of African Caribbean ancestry: Tobago women's health study. Bone 2008;43:156–61. [PubMed: 18448413]
32. Kuipers A, Zhang Y, Cauley JA, Nestlerode CS, Chu Y, Bunker CH, Patrick AL, Wheeler VW, Hoffman AR, Orwoll ES, Zmuda JM. Association of a high mobility group gene (HMGA2) variant with bone mineral density. Bone 2009;45:295–300. [PubMed: 19376282]
33. Devlin B, Risch N. A comparison of linkage disequilibrium measures for fine-scale mapping. Genomics 1995;29:311–22. [PubMed: 8666377]
34. Stephens M, Smith NJ, Donnelly P. A new statistical method for haplotype reconstruction from population data. Am J Hum Genet 2001;68:978–89. [PubMed: 11254454]
35. Hartmann C, Tabin CJ. Dual roles of Wnt signaling during chondrogenesis in the chicken limb. Development 2000;127:3141–59. [PubMed: 10862751]
36. Blais A, Dynlacht BD. E2F-associated chromatin modifiers and cell cycle control. Curr Opin Cell Biol 2007;19:658–62. [PubMed: 18023996]
37. Giangrande PH, Hallstrom TC, Tunyaplin C, Calame K, Nevins JR. Identification of E-box factor TFE3 as a functional partner for the E2F3 transcription factor. Mol Cell Bio 2003;23:3707–20. [PubMed: 12748276]
38. Schlisio S, Halperin T, Vidal M, Nevins JR. Interaction of YY1 with E2Fs, mediated by RYBP, provides a mechanism for specificity of E2F function. EMBO J 2002;21:5775–86. [PubMed: 12411495]
39. Wu L, Timmers C, Maiti B, Saavedra HI, Sang L, Chong GT, Nuckolls F, Giangrande P, Wright FA, Field SJ, Greenberg ME, Orkin S, Nevins JR, Robinson ML, Leone G. The E2F1-3 transcription factors are essential for cellular proliferation. Nature 2001;414:457–62. [PubMed: 11719808]
40. Humbert PO, Verona R, Trimarchi JM, Rogers C, Dandapani S, Lees JA. E2f3 is critical for normal cellular proliferation. Genes Dev 2000;14:690–703. [PubMed: 10733529]

41. Tsai SY, Opavsky R, Sharma N, Wu L, Naidu S, Nolan E, Feria-Arias E, Timmers C, Opavska J, de Bruin A, Chong JL, Trikha P, Fernandez SA, Stromberg P, Rosol TJ, Leone G. Mouse development with a single E2F activator. Nature 2008;454:1137–41. [PubMed: 18594513]
42. Scheijen B, Bronk M, van der Meer T, Bernards R. Constitutive E2F1 overexpression delays endochondral bone formation by inhibiting chondrocyte differentiation. Mol Cell Biol 2003;23:3656–68. [PubMed: 12724423]
43. Hughes TA, Brady HJ. Cross-talk between pRb/E2F and Wnt/beta-catenin pathways: E2F1 induces axin2 leading to repression of Wnt signalling and to increased cell death. Exp Cell Res 2005;303:32–46. [PubMed: 15572025]
44. Lacroix AZ, Beck TJ, Cauley JA, Lewis CE, Bassford T, Jackson R, Wu G, Chen Z. Hip structural geometry and incidence of hip fracture in postmenopausal women: what does it add to conventional bone mineral density? Osteoporos Int. 2009
45. Szulc P. Bone density, geometry, and fracture in elderly men. Curr Osteoporos Rep 2006;4:57–63. [PubMed: 16822404]
46. Melton LJ 3rd, Riggs BL, Keaveny TM, Achenbach SJ, Hoffmann PF, Camp JJ, Rouleau PA, Bouxsein ML, Amin S, Atkinson EJ, Robb RA, Khosla S. Structural determinants of vertebral fracture risk. J Bone Miner Res 2007;22:1885–92. [PubMed: 17680721]
47. Kim JG, Kim H, Jee BC, Suh CS, Choi YM, Moon SY. Non-association between polymorphisms of the frizzled receptor genes and bone mineral density in postmenopausal Korean women. J Korean Med Sci 2009;24:443–7. [PubMed: 19543507]
48. Richards JB, Rivadeneira F, Inouye M, Pastinen TM, Soranzo N, Wilson SG, Andrew T, Falchi M, Gwilliam R, Ahmadi KR, Valdes AM, Arp P, Whittaker P, Verlaan DJ, Jhamai M, Kumanduri V, Moorhouse M, van Meurs JB, Hofman A, Pols HA, Hart D, Zhai G, Kato BS, Mullin BH, Zhang F, Deloukas P, Uitterlinden AG, Spector TD. Bone mineral density, osteoporosis, and osteoporotic fractures: a genome-wide association study. Lancet 2008;371:1505–12. [PubMed: 18455228]
49. Styrkarsdottir U, Halldorsson BV, Gretarsdottir S, Gudbjartsson DF, Walters GB, Ingvarsson T, Jonsdottir T, Saemundsdottir J, Center JR, Nguyen TV, Bagger Y, Gulcher JR, Eisman JA, Christiansen C, Sigurdsson G, Kong A, Thorsteinsdottir U, Stefansson K. Multiple genetic loci for bone mineral density and fractures. N Engl J Med 2008;358:2355–65. [PubMed: 18445777]
50. Rivadeneira F, Styrkarsdottir U, Estrada K, Halldorsson BV, Hsu YH, Richards JB, Zillikens MC, Kavvoura FK, Amin N, Aulchenko YS, Cupples LA, Deloukas P, Demissie S, Grundberg E, Hofman A, Kong A, Karasik D, van Meurs JB, Oostra B, Pastinen T, Pols HA, Sigurdsson G, Soranzo N, Thorleifsson G, Thorsteinsdottir U, Williams FM, Wilson SG, Zhou Y, Ralston SH, van Duijn CM, Spector T, Kiel DP, Stefansson K, Ioannidis JP, Uitterlinden AG. Twenty bone-mineral-density loci identified by large-scale meta-analysis of genome-wide association studies. Nat Genet. 2009
51. Styrkarsdottir U, Halldorsson BV, Gretarsdottir S, Gudbjartsson DF, Walters GB, Ingvarsson T, Jonsdottir T, Saemundsdottir J, Snorradottir S, Center JR, Nguyen TV, Alexandersen P, Gulcher JR, Eisman JA, Christiansen C, Sigurdsson G, Kong A, Thorsteinsdottir U, Stefansson K. New sequence variants associated with bone mineral density. Nat Genet 2009;41:15–7. [PubMed: 19079262]
52. Xiong DH, Liu XG, Guo YF, Tan LJ, Wang L, Sha BY, Tang ZH, Pan F, Yang TL, Chen XD, Lei SF, Yerges LM, Zhu XZ, Wheeler VW, Patrick AL, Bunker CH, Guo Y, Yan H, Pei YF, Zhang YP, Levy S, Papasian CJ, Xiao P, Lundberg YW, Recker RR, Liu YZ, Liu YJ, Zmuda JM, Deng HW. Genome-wide association and follow-up replication studies identified ADAMTS18 and TGFBR3 as bone mass candidate genes in different ethnic groups. Am J Hum Genet 2009;84:388–98. [PubMed: 19249006]

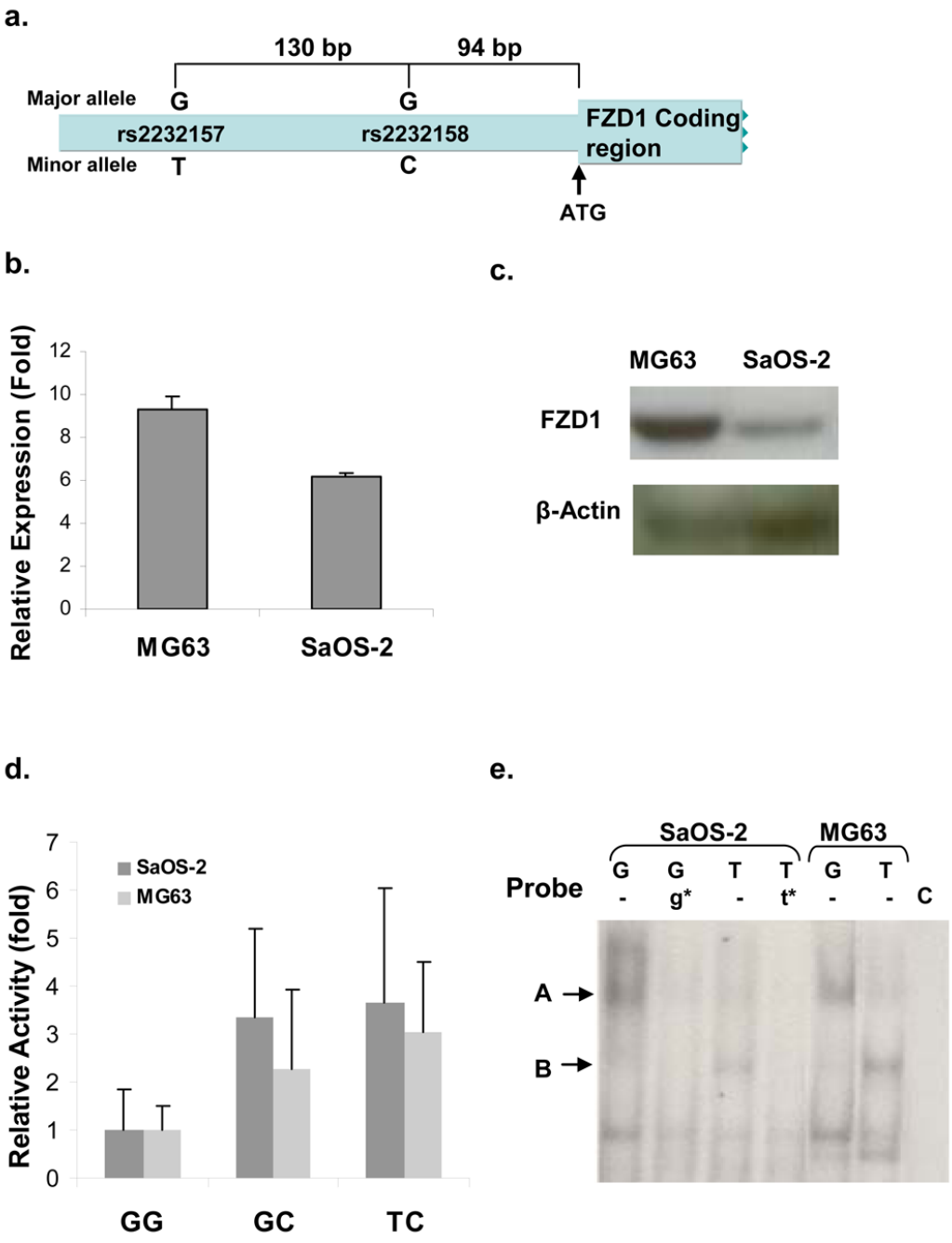

Figure 1.

a) Schematic of the *FZD1* 5′ UTR region. The relative locations of rs2232157 and rs 2232158 are shown. b) Quantitative RT-PCR analysis of FZD1. Relative expression level (ΔCt) was calculated using ΔCt of GAPDH as a reference. c). Western blot analysis of FZD1 protein in MG63 and SaOS-2 cells. Beta-actin was used as an internal control to demonstrate protein loading. d) Activity of the haplotype specific *FZD1* promoters. The promoter activity for different *FZD1* haplotypes were assessed by transfecting MG63 and SaOS-2 cell lines with luciferase reporter plasmids. Differences in activity were tested using the Kruskal-Wallis and Wilcoxon rank sum test. e) Allele specific binding to the rs2232157 specific probes by nuclear proteins. EMSA was carried out using radio-labeled probes for the two alleles of rs2232157

with nuclear extracts from both MG63 and SaOS-2 cells. The two major complexes are labeled with A and B. To ensure specificity of binding, the reaction was incubated with 50-fold excess unlabeled G and T probes (denoted by g* and t*, respectively). As a control, binding reaction with radio-labeled probe without nuclear extract was conducted (denoted as C).

Table 1

Characteristics of the 1321 Genotyped Afro-Caribbean Men

Trait	Mean (SD) or Frequency
Age (years)	59.8 (10.5)
Height (cm)	174.8 (6.9)
Weight (kg)	84.28 (16.1)
BMI (kg/m^2)	27.5 (4.8)
rs2232157 minor allele (T)	21.4%
rs2232158 minor allele (C)	33.9%
GG haplotype	71.8%
GC haplotype	6.9%
TC haplotype	21.3%

Table 2

FZD1 Genotype Associations with Femoral Neck BMD and Geometry in Afro-Caribbean Men

	Genotype Mean (SE)			
Trait	**1/1**	**1/2**	**2/2**	**p-value***
rs2232157	N=824	N=422	N=70	
BMD (g/cm^2)	1.053 (0.005)	1.045 (0.007)	1.050 (0.018)	0.438
Cross-sectional Area (cm^2)	3.170 (0.015)	3.181 (0.021)	3.185 (0.051)	0.636
Subperiosteal Width (cm)	3.172 (0.007)	3.200 (0.010)	3.194 (0.024)	**0.017**
Cross-sectional Moment of Inertia (cm^4)	2.693 (0.018)	2.758 (0.025)	2.748 (0.061)	**0.030**
rs2232158	N=556	N=629	N=132	
BMD (g/cm^2)	1.046 (0.007)	1.053 (0.006)	1.050 (0.013)	0.431
Cross-sectional Area (cm^2)	3.178 (0.018)	3.170 (0.017)	3.176 (0.037)	0.765
Subperiosteal Width (cm)	3.196 (0.009)	3.171 (0.008)	3.182 (0.018)	**0.038**
Cross-sectional Moment of Inertia (cm^4)	2.748 (0.022)	2.688 (0.020)	2.722 (0.044)	0.059

* all p-values are from the dominant model (best fit) adjusted for age, height and weight 1, major allele; 2, minor allele. SE, standard error of the mean.

Table 3

FZD1 Haplotype Associations with Femoral Neck BMD and Geometry in Afro-Caribbean Men

	Haplotype Mean (SE)			
Trait	**0**	**1**	**2**	**p-value***
GG	N=119	N=506	N=692	
BMD (g/cm^2)	1.034 (0.014)	1.050 (0.007)	1.053 (0.006)	0.221^d
Cross-sectional Area (cm^2)	3.133 (0.039)	3.192 (0.019)	3.169 (0.016)	0.272^d
Subperiosteal Width (cm)	3.191 (0.019)	3.197 (0.009)	3.171 (0.008)	**0.026** ^{r}
Cross-sectional Moment of Inertia (cm^4)	2.709 (0.047)	2.758 (0.023)	2.688 (0.019)	**0.031** ^{r}
GC	N=1140	N=172	N=5	
BMD (g/cm^2)	1.052 (0.005)	1.040 (0.012)	1.036 (0.069)	0.329^d
Cross-sectional Area (cm^2)	3.179 (0.013)	3.142 (0.033)	3.172 (0.191)	0.292^d
Subperiosteal Width (cm)	3.183 (0.006)	3.181 (0.015)	3.220 (0.090)	0.949^d
Cross-sectional Moment of Inertia (cm^4)	2.720 (0.015)	2.694 (0.039)	2.808 (0.228)	0.591^d
TC	N=825	N=422	N=70	
BMD (g/cm^2)	1.052 (0.005)	1.045 (0.007)	1.050 (0.018)	0.456^d
Cross-sectional Area (cm^2)	3.170 (0.015)	3.182 (0.021)	3.185 (0.051)	0.618^d
Subperiosteal Width (cm)	3.172 (0.007)	3.200 (0.010)	3.194 (0.024)	**0.018** ^{d}
Cross-sectional Moment of Inertia (cm^4)	2.693 (0.018)	2.758 (0.025)	2.749 (0.061)	**0.029** ^{d}

0, zero copies of the haplotype; 1, one copy of the haplotype; 2, two copies of the haplotype. SE, standard error of the mean.

*p-values of the best fit model adjusted for age, height and weight are shown:

^{d}dominant model;

^{r}recessive model